Freestanding Micro-Supercapacitor With Interdigital Electrodes for Low-Power Electronic Systems

Yu Song, Xue-Xian Chen, Jin-Xin Zhang, Xiao-Liang Cheng, and Hai-Xia Zhang, *Senior Member, IEEE*

***Abstract*— With the rapid development of miniaturized multi-functional systems, micro-energy-storage devices have drawn increasing attention due to the importance of power supply. In this paper, a novel fabrication for freestanding solid-state micro-supercapacitors (MSCs) has been proposed and developed by combining electrolyte transferring with laser patterning process. Typical freestanding MSC is composed of interdigital carbon nanotube/nanofibers as active material employed by laser patterning process, PVA/H_3PO_4 as both the solid-state electrolyte and the flexible substrate, and gold layer as the current collector. With the in-planar electrode and electrolyte-substrate layout, the dimension of the MSC could be greatly decreased without excess substrate. Taking advantage of electrospinning nanofibers with large surface area and carbon nanotubes with high conductivity, we optimize the line-width (200 μm) of the interdigital finger of the MSC, which exhibits high areal capacitance (15.6 mF/cm^2) and excellent cycling stability. With the serial design, the working range of MSC units could be greatly enhanced in wearable devices and low-power electronic systems. Therefore, such flexible MSC is a promising candidate to satisfy the requirements of miniaturized energy systems. [2017-0059]**

***Index Terms*— Micro supercapacitor, freestanding, laser patterning, electrolyte transferring, interdigital.**

I. Introduction

THE CURRENT developments of integrated electronics and portable devices have raised the demands for rechargeable microscale power sources of appropriate size and stable performance [1], [2]. With the rapid growth of various energy technology, micro energy-storage units are especially important for integrating energy conversion devices [3]–[8], such as triboelectric nanogenerator, piezoelectric nanogenertor, electromagnetic energy harvester and other electronic circuits to build a self-powered microsystem [9], [10]. Among the presently available energy storage devices [11]–[13], supercapacitors are a promising state-of-the-art device, filling the blank between the battery with high specific energy density and the conventional capacitor with high specific power density. Supercapacitors have advantages of long cycle lifetime, fast charging/discharging rate and wide operating temperature ranges [13], [14]. These properties make supercapacitors serving as crucial component to build advanced energy systems [15], [16].

Unfortunately, sandwiched structure of the conventional supercapacitor limits its applications in on-chip device and microsystem [17], [18], because the miniaturized electronics and mechanical devices desire energy components with similar dimensions compared with other elements to form self-powered system. Furthermore, microscale and on-chip energy storage devices can achieve high ratio of energy delivery at high charging/discharging rates due to a shortened diffusion length. Therefore, the in-planar supercapacitor, also called micro-supercapacitor (MSC) [19], has drawn great attentions in micro energy fields. As an emerging member in the family of the supercapacitor, such in-planar layout can render the diffusion length and promote the procedure of ion exchange [20]–[22]. Independent to the electrode thickness, MSC could allow more active materials loaded per unit and maintain excellent electrochemical performance at the same time. In addition, owing to the in-planar layout and elimination of the separator, the total thickness of the device could be great decreased, enabling the integration of power sources to the electronic circuit [23], [24].

Recently, several researches make considerable contributions to enhancing the energy density, reliably and cycling stability of the MSC by utilizing different active nanomaterials [25] and developing advanced structures [26]. On one hand, carbon-based materials such as carbon nanotubes (CNTs) [27], graphene [28] and activated carbons [29] have been widely used. On the other hand, solid-state electrolytes are employed [30], which broadening the applications of the MSC with flexibility in wearable and portable devices. However, most of the works mainly focused on the performance improvement of the MSC, and ignored the cost, ease of preparation and device integration, which are quite important in micro energy fields [31]. For example, due to the fact that the patterning of the interdigital MSC are commonly employed with lithography process [32], it has proved costly and awkward in developing energy storage devices, which could possibly damage and corrode the electrode materials during the etching stage. These processes lead to a complicated fabrication and limit the performance of the flexible devices. Moreover, in order to ensure the flexibility, the electrodes need to be transferred from a rigid substrate to a flexible substrate,

Manuscript received March 16, 2017; revised April 29, 2017; accepted May 14, 2017. Date of publication June 4, 2017; date of current version September 29, 2017. This work was supported in part by the National Natural Science Foundation of China under Grant 61674004, Grant 61176103, and Grant 91323304; in part by the National Key Research and Development Project from the Minister of Science and Technology, China, under Grant 2016YFA0202701; in part by the Beijing Science and Technology Project under Grant D151100003315003; and in part by the Beijing Natural Science Foundation of China under Grant 4141002. Subject Editor P. M. Sarro. *(Corresponding author: Hai-Xia Zhang.)*

The authors are with the Institute of Microelectronics, Peking University, Beijing 100871, China (e-mail: songyupku@pku.edu.cn; xxchen@pku.edu.cn; zjxpku@pku.edu.cn; xlcheng@pku.edu.cn; zhang-alice@pku.edu.cn).

Color versions of one or more of the figures in this paper are available online at http://ieeexplore.ieee.org.

Digital Object Identifier 10.1109/JMEMS.2017.2705130

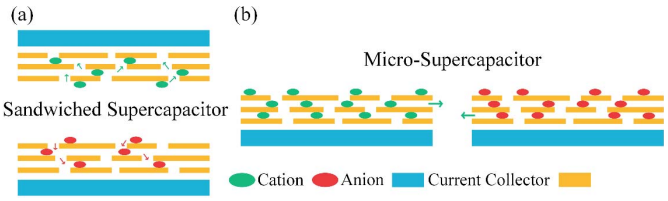

Fig. 1. Schematic illustration of the longer ion transfer distance and incomplete utilization of surface area in (a) stacked SC, and shorter ion transfer distance and complete utilization of surface in (b) interdigital MSC.

which brings in excess substrate to further increase the whole thickness and destroys the device integrity to some extent [33]. Therefore, it remains a challenge to fabricate MSC with excellent stability, flexibility in a low-cost and easy process at the same time.

To address the above issues, based on our previous work [34], we have presented an interdigital freestanding MSC through the electrolyte transferring and laser patterning process as a solution to fabricate the flexible and on-chip energy storage device. In our design, the gel electrolyte serves as both ion reservoir and flexible substrate, which could reduce the total thickness and enhance the flexibility without excess substrate. Meanwhile, without the lithography and use of shadow mask, the interdigital structure could be facilely obtained with the controllable laser-patterning process, which could simplify the scalable and low-cost fabrication. Additionally, taking advantage of the electrospinning nanofibers with large surface area and CNTs with high conductivity, we could optimize the line-width of the MSC unit which exhibits high areal capacitance and stability. The working range of the MSC could be further improved through the serial design and drive low-power device reliably. Therefore, such flexible freestanding MSC shows great potentials in wearable devices and has significant impact on the low-power electronic systems.

II. Device

A. Device Configuration

For the conventional sandwiched supercapacitor, the surfaces of active materials are incompletely utilized and the electrolyte ions need to transfer a longer distance since the materials are stacked in parallel to the current collector, as illustrated in Fig. 1(a). Compared with the stacked structure, MSC with in-planar layout (Fig. 1(b)) forming alternate interdigital electrodes shows several advantages. The electrolyte ions can transfer along the interspace of active materials which could shorten the transfer path and maximize the utilization of the electrochemical surfaces, resulting in the higher capacitance and better rate performance. Furthermore, with the distance between adjacent electrodes precisely controlled in small scale, the device configuration is promising to be extended in the third dimension, and making full use of the limited on-chip space. Therefore, the in-planar MSC could be developed with compatible and scalable fabrication process and integrated with low-power electronics and wearable devices.

The freestanding solid-state MSC device is designed as shown in Fig. 2, which includes the nanofibers,

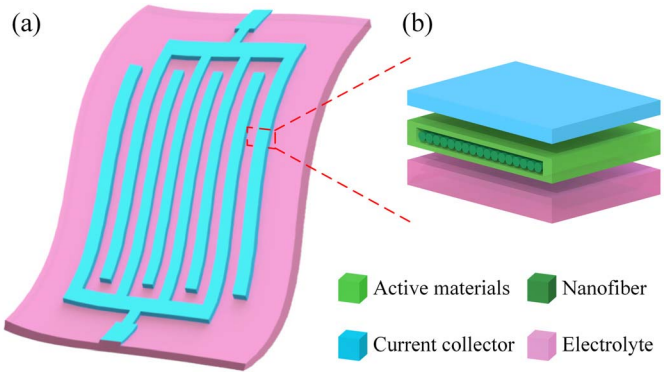

Fig. 2. Schematic diagram of the freestanding MSC. (a) Flexible view of the device, and (b) exploded view of the interdigital structure.

active materials, current collector and solid-state electrolyte. At first, the active materials should have good electrochemical properties, high conductivity and mechanical strength to build up 3D electrodes, such as carbon nanotubes and graphene. Meanwhile, nanofiber network that is highly porous, providing pathway for ion transport. Nanofibers also own high surface area for the active materials, showing capability for the substrate of the electrodes. Herein, we choose electrospinning, a general method to obtain nanofibers, with drop-drying process of active materials to meet the demands of high performance electrodes, where the active materials are densely coated on the nanofibers with large surface area and high conductivity. Then the gel electrolyte plays the role of both the ion reservoir and solid substrate, which could decrease the whole device's thickness and simplify the fabrication process. The gel electrolyte with active materials forms the 3D electrolyte/electrode structure as the flexible and robust substrate. A metal layer on the top layer serves as current collector to enhance the ion transport and protect the active materials. Finally, considering the fact that laser patterning process owns low cost and high precision features, the interdigital electrodes could be obtained without further etching stage.

B. Measurement and Analysis

The interdigital structure of the MSC is observed by an optical microscopy (CX22, Nikon Co.). The morphological characteristic of each layer and the interdigital MSC are investigated by scanning electron microscopy (SEM, Quanta 600F, FEI Co., 20 kV). As for the electrochemical tests, after the fabrication of MSCs, the contact pads of each electrode are connected with aluminum foil using silver paste. Cyclic voltammetry (CV), galvanostatic charging/discharging (GCD) and electrochemical cycling stability of the freestanding MSC devices under an in-planar configuration with gel electrolyte are carried out with a two-electrode system using electrochemical workstation (CHI660C, CH instrument) at room temperature.

III. Experiments

A. Materials Preparation

As we know, the preparation of the polymer solution is essential for the electrospinning process. In our process,

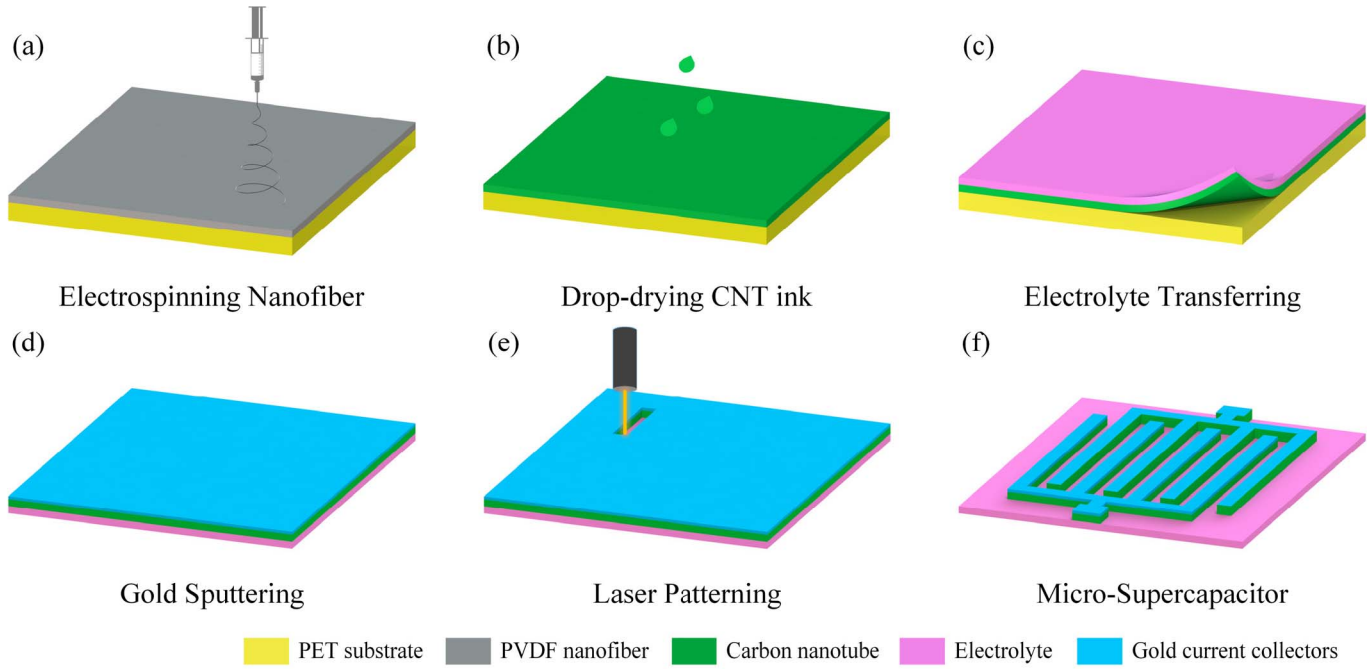

Fig. 3. 3D schematic of the fabrication process of the freestanding MSC. (a) Depositing PVDF nanofibers on the PET substrate through electrospinning process; (b) drop-drying CNT ink on the nanofibers as the active materials; (c) spray-coating electrolyte and transferring the electrodes by the electrolyte from the substrate; (d) sputtering the gold layer as the current collector; (e) patterning the electrode and current collector with the laser cutting process, and (f) obtaining the interdigital MSC device.

1 g of polyvinylidene fluoride (PVDF, Kureha) is dissolved in dimethyl formamide (DMF)/acetone (Sigma Aldrich) mixtures at a polymer/solvent concentration of 10% w/w and the mixture is subsequently magnetic stirred for 8 h at the room temperature until the solution becomes homogeneous and transparent. To optimize the electrospinning conditions, we use different solvents such as butanone and dimethyl sulfoxide with different proportions. We have found that the addition of DMF is crucial for the continuous electrospinning process, because DMF has a slower evaporation speed than acetone or butanone and avoid the clogging of the needle. The CNT ink solution is developed by dispersing 60 mg of CNTs with 60 mg of sodium dodecylbenzenesulfonate (SDBS) surfactant in 60 ml of deionized water. To disperse evenly, the solution is bath-sonicated for 4 h. In addition, the solid-state polyvinyl alcohol/phosphoric acid (PVA/H_3PO_4) gel electrolyte is prepared by mixing PVA powder (6 g) into H_3PO_4 aqueous solution (6 g H_3PO_4 into 60 ml deionized water). The whole mixture is heated to 85°C under magnetic stirring until the solution becomes clear.

B. Fabrication Process

The fabrication process of the MSC device is demonstrated in Fig. 3. Firstly, to obtain PVDF nanofibers with large surface area, electrospinning process is performed by placing 0.9 ml of PVDF solution into a 1.0 ml plastic syringe with a blunt-tip needle. With the needle placed 8 cm away from the collector and charged at a bias voltage of 10 kV, the solution is fed up at a constant speed of 1 ml/h. Under such high voltage, the polymer solution is ejected and finally collected by the substrate (Fig. 3(a)). The detailed operating parameters are listed in Table. 1.

TABLE I
OPERATING PARAMETERS FOR PVDF NANOFIBER ELECTROSPINNING

Parameters	Value
Powder concentration	10 wt%
Solvent (DMF: acetone) weight ratio	2:8-5:5
Applied voltage	10 kV
Needle-to-collector distance	8 cm

Then CNT ink solution is dropped on the nanofibers and dried at 90°C for several times until the CNT is saturated among the nanofibers as the active materials, leading to a CNT density of 0.2 mg/cm^2 (Fig. 3(b)). Next, gel electrolyte consisting of PVA and H_3PO_4 is spray coated on the CNT-nanofiber electrodes. The device is completely dried in a regular oven at 45°C for 12 h to fully vaporize the excess water. After the above layers are peeled off from the PET substrate mechanically, the electrodes are easily transferred to the electrolyte film without further substrate (Fig. 3(c)).

To efficiently promote the charge flow, Au (100 nm) is sputtered beyond the electrodes as current collector via magnetron sputtering process (Fig. 3(d)). Using the laser cutting machine (GKNQL-355, Beijing Guoke Laser Co.), the electrodes and current collector could be patterned into designed interdigital structure together (Fig. 3(e)). The detailed parameters of the laser-patterning process are listed in Table. 2. Finally, the freestanding solid-state MSC is successfully fabricated and each single device weighs only 20 mg, which performs

TABLE II
OPERATING PARAMETERS FOR LASER-PATTERNING PROCESS

Parameters	Value
Power (W)	3
Field lens (mm)	160
Velocity (mm/s)	1000
Pulse width (μs)	1
Corner delay (μs)	100
Cycle	20
Frequency (kHz)	30

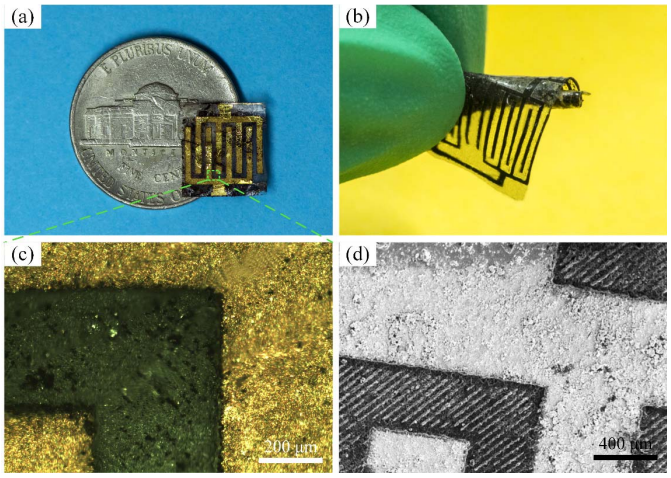

Fig. 4. Photograph of the (a) MSC device placed on a coin and (b) in twisted condition with high flexibility. (c) Microscopic image and (d) SEM image of the interdigital structure of the MSC device with well-defined shape and sharp boundaries.

excellent flexibility and portability and is easily integrated with low-power electronic systems and flexible circuits (Fig. 3(f)).

C. Characterization

Using the proposed process, the freestanding MSC with patterned electrodes has been fabricated. Fig. 4(a) shows prototype of the device placed on a coin, the volume of which is 1 cm × 1 cm × 300 μm. In addition, Fig. 4(b) demonstrates a digital photograph of the MSC bended omnidirectionally to the interdigital electrodes by the finger, indicating good flexibility and excellent mechanical stability of the MSC. From the optical microscopic image in Fig. 4(c) and SEM image in Fig. 4(d), both of them clearly illustrate that the electrodes of the MSC have a well-defined shape and sharp boundaries. The whole device also proves the uniform laser-cutting process, where the current collector and the electrodes are patterned into the designed interdigital structure instead of the electrolyte-substrate.

Fig. 5 gives more information about the morphologies of the prototypes and materials. As shown in the SEM image of Fig. 5(a), with the electrospinning time increasing, the nanofibers would stack layer by layer and own large surface area. In Fig. 5(b), SEM image with high magnification shows the CNTs are densely coated among the nanofibers after several drop-drying process, which form the conductive

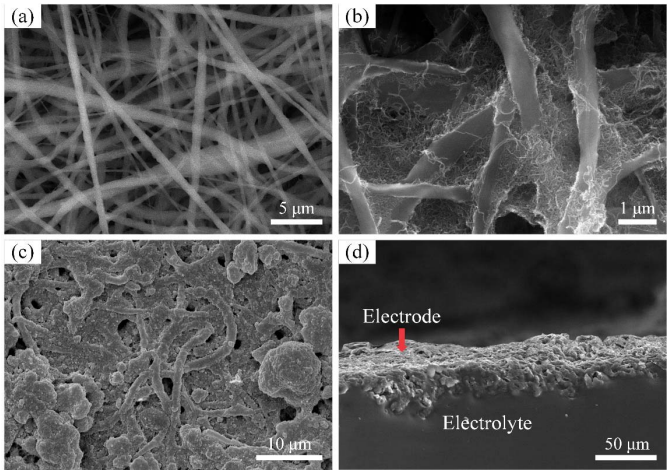

Fig. 5. SEM image of (a) electrospinning nanofibers, (b) CNT densely coated nanofibers, (c) gold sputtered electrodes uniformly and (d) the cross-section of the electrolyte/electrode structure.

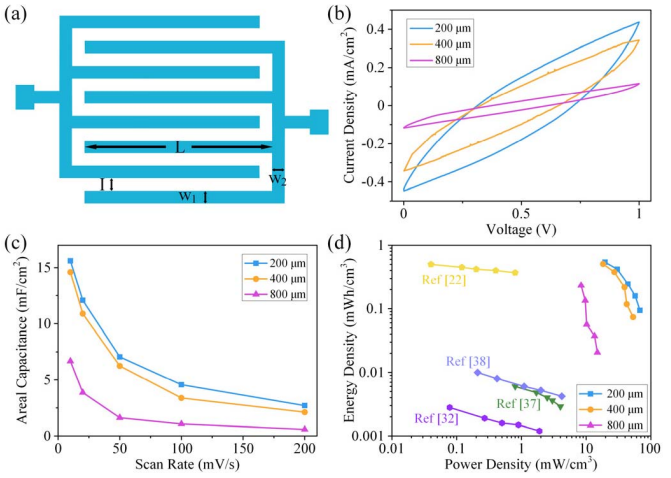

Fig. 6. (a) Interdigital structure of designed MSC with different parameters. Electrochemical performance of MSC 200, MSC 400, MSC 800: (b) cyclic voltammetry, (c) areal capacitance and (d) Ragone plots.

network with the high conductivity. SEM image in Fig. 5(c) demonstrates that the conformal gold layer is deposited as the top layer. It works as current collector to improve the ion transport. The cross-section of the freestanding MSC (SEM image in Fig. 5(d)) reveals the compact structure of the electrode/electrolyte, which predicts good electrochemical stability of the MSC. Additionally, the thickness of the electrode materials is about 40 μm. It is worth noting that the electrolyte is penetrated into the electrode, thus enhancing the ion exchange greatly.

IV. RESULTS & DISCUSSION

A. Electrochemical Performance

To investigate the relationship between electrochemical performance and the line-width, MSCs with 200, 400, and 800 μm line-width of finger (defined as MSC 200, MSC 400, and MSC 800) are designed. The schematic diagram in Fig. 6(a) stands for a MSC unit and the meanings of each symbol, where each interdigital electrode has four fingers.

TABLE III
DETAILED PARAMETERS FOR DESIGNED INTERDIGITAL MSC UNIT

Parameters	MSC 200	MSC 400	MSC 800
W_1 (μm)	200	400	800
W_2 (μm)	200	400	800
I (μm)	400	400	400
L (μm)	6000	6000	6000
Total area (cm^2)	0.1328	0.2552	0.5336
Total volume (10^{-4} cm^3)	5.312	10.208	21.344

Table. 3 includes the detailed parameter of each symbol, where each MSC unit owns different area and volume and the interspace of interdigital finger is kept for a value of 400 μm.

At first, CV curves of MSC 200, MSC 400, and MSC 800 at a scan rate of 100 mV/s with a potential window of 0–1 V are recorded (Fig. 6(b)). Quasi-rectangular shapes could be observed due to the characteristic of the carbon-based materials, indicating the ideal double-layer electrochemical behavior. As the areal capacitance is the most precise characterization for evaluating the charge-storage capacity of MSC, it is analyzed according to the following Equation (1) with the CV curves of these freestanding MSCs: [35]

$$C_A = \frac{Q}{A \cdot \Delta V} = \frac{1}{\mathrm{k} \cdot A \cdot \Delta V} \int_{V_1}^{V_2} I(V)\mathrm{d}V, \tag{1}$$

where C_A is the areal capacitance, $I(V)$ is the discharge current function, k is the scan rate, A is the area of the MSC. Additionally, ΔV is the potential window during the discharge process, where V_1 and V_2 are maximum and minimum voltage values, respectively. With the scan rate of 10 mV/s, the MSC 200 could achieve the maximum areal capacitance of 15.6 mF/cm^2, which is definitely higher than MSC 400 (14.6 mF/cm^2) and MSC 800 (6.8 mF/cm^2), indicating the areal capacitance increases as the interdigital finger line-width is decreased. Meanwhile, the areal capacitance decreases slightly with the increase of the scan rate (Fig. 6(c)). As a result, MSCs could withstand the charging-discharging process without significant degradation in areal capacitance even at high scan rate, showing a stable and excellent electrochemical performance.

We suggest that the shorten line-width reduce the ions and charge transport path to make use of active materials completely and improve rate capability. The pathway of ions transport from one electrode to the counted electrode is obviously shortened as the line-width decreases. As a result, a high capacitance and fast charge-discharge rate performance are achieved, which show continuously increasing with a decrease in line-width. Additionally, as for energy storage devices, how much charges could be stored and how quickly the charges could be stored and released are very important for their applications. Therefore, energy density and power density (Ragone plots) are other key metrics for evaluating the different types of energy storage devices [36]. The volumetric energy and power density of all MSCs are calculated from

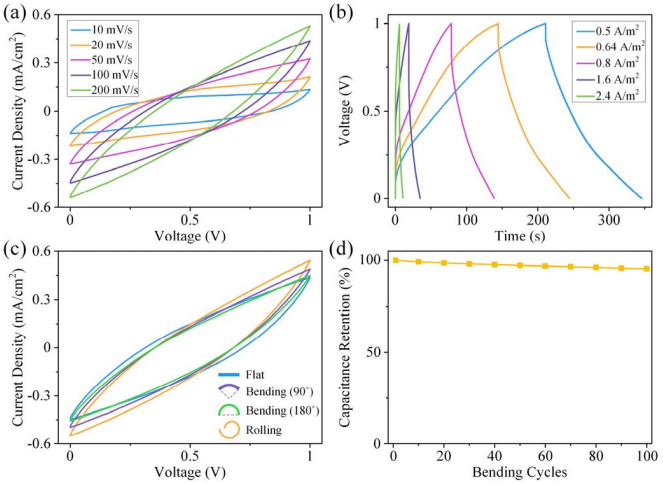

Fig. 7. Electrochemical performance of the optimized MSC 200, (a) cyclic voltammetry curves at different scan rates, (b) galvanostatic charging-discharging curves at different current densities, (c) cyclic voltammetry curves under different bending and rolling state at the scan rate of 100 mV/s and (d) capacitance stability under several bending cycle.

CV curves at a voltage scan rate of 10 to 200 mV/s, and shown in Fig. 6(d). Both of the energy and power density of these MSCs at initial state could be achieved by the following Equations (2)-(4) with different volumes: [35]

$$C_V = \frac{Q}{V \cdot \Delta V} = \frac{1}{\mathrm{k} \cdot V \cdot \Delta V} \int_{V_1}^{V_2} I(V)\mathrm{d}V \tag{2}$$

$$E = \frac{1}{2 \times 3600} C_V (\Delta V)^2 \tag{3}$$

$$P = \frac{E}{\Delta t} \times 3600, \tag{4}$$

where V is the volume of the MSC, C_V is the volumetric capacitance of the MSC which can be achieved through (2), Δt is the discharging time, E is the energy density and P is the power density, respectively. Compared to other energy storage devices, MSC 200 can obtain a maximum power density (67.7 mW/cm^3) at the scan rate of 200 mV/s. As the scan rate changes to 10 mV/s, it can continue to maintain high energy density (0.54 mWh/cm^3). In addition, MSC 400 and MSC 800 can also maintain high-specific energy and power as shown in Ragone plots. Definitely, both of them vary slightly with the increase of scan rates. The results reveal that these MSCs possess good capability in delivering energy.

B. Analysis of MSC 200

Afterwards, in order to further explore the electrochemical performance of the MSC 200 with optimized line-width, the device is carefully evaluated through CV, GCD and cycling stability tests via the electrochemical workstation. With the effective area of 0.1328 cm^2, the MSC 200 is analyzed by CV curves with the scan rates from 10 mV/s to 200 mV/s at a stable potential window of 0–1 V (Fig. 7(a)). Definitely, the CV curves retain quasi-rectangular shape and are approximately symmetrical about the zero-current line, thus indicating the ideal double-layer electrochemical behavior.

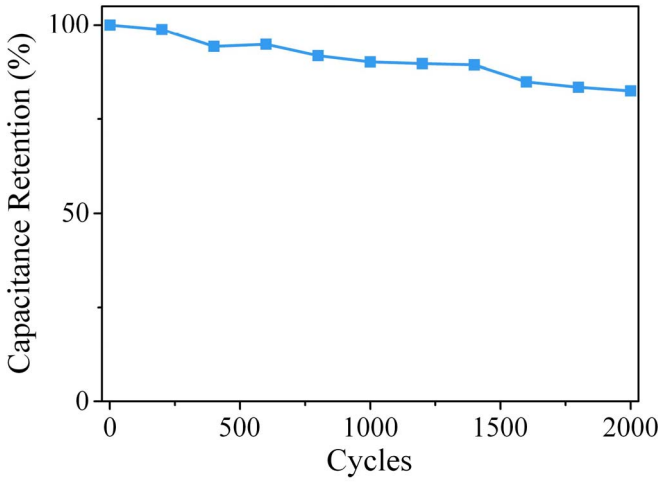

Fig. 8. Cycling stability of the MSC 200 at the first 2,000 charging-discharging cycles.

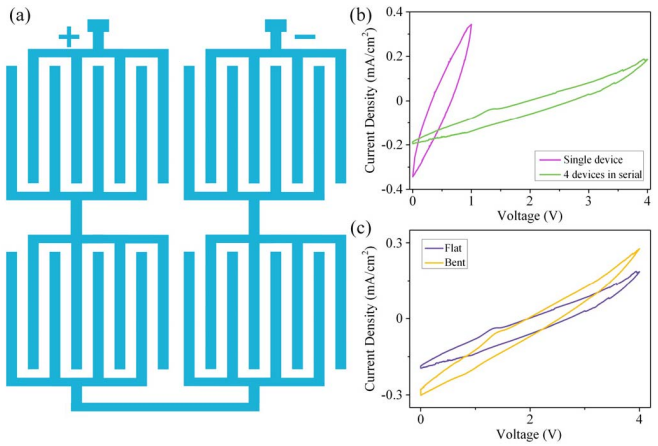

Fig. 9. (a) The circuit diagram of the four MSC 400 units connected in serial. (b) Cyclic voltammetry curves of serial MSC 400 units compared with the single MSC 400 unit and flexible tests of the performance.

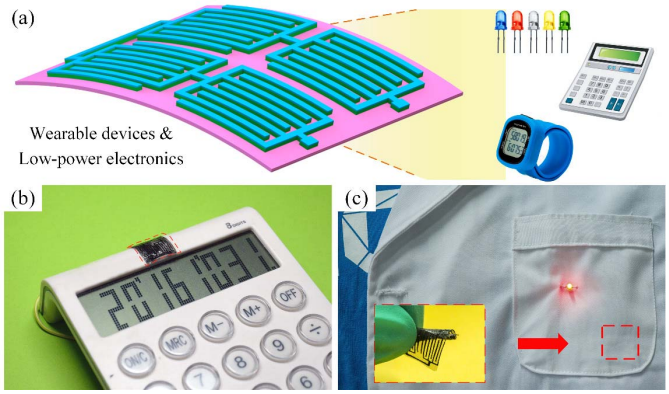

Fig. 10. (a) Serial MSC units show potentials in wearable devices and low-power electronic systems. (b) Commercial calculator and (c) wearable LED could be driven stably with the serial MSC units placed on the bent surface or coat pocket.

Then GCD test is also carried out to further evaluate the electrochemical performance of MSC 200. As shown in Fig. 7(b), the typical GCD curves are performed, the charging-discharging current densities of which are from 0.5 A/m^2 to 2.4 A/m^2. Discharging profiles of the fabricated MSC 200 are dependent on the applied charging-discharging current densities and similar curve shapes have been obtained for different current densities. Evidently, GCD curves could reveal that all of the charging curves are relatively symmetrical with their corresponding discharging counterparts, as well as their excellent linear voltage-time profiles, demonstrating good electrochemical behavior of the device.

In order to evaluate the feasibility as energy storage component for flexible electronics, the MSC device is tested under various bending or rolling state at the scan rate of 100 mV/s. From Fig. 7(c), there are negligible changes of the CV curves under different bending and rolling states, which greatly proves excellent flexibility of the MSC device. Furthermore, under repeated bending cycles, the electrochemical performance is nearly not altered shown in Fig. 7(d), convincing the remarkable stability of the device.

Fig. 8 shows the capacitance retention of the MSC 200 with interdigital electrodes during the repetitive charge/discharge cycles (100 mV/s). It is obvious that about 83% of the initial capacitance is maintained after 2,000 cycles of CV tests. Therefore, the cycling stability and relative electrochemical tests of the MSCs indicate that the freestanding device owns stable and excellent electrochemical performance, which could satisfy the needs of the flexible electronics and self-powered systems.

C. Serial MSC Units

Since a single MSC device has limited working potential window and energy storage capacity, to meet the demands of various applications, the serial connecting circuit of flexible MSC units is studied and explained in detail. Taking the electrochemical performance and device robustness into account, we utilize the MSC 400 for serially connected array that possesses the good capability in delivering energy and shows good stability at the same time. Fig. 9(a) illustrates the schematic of four MSC 400 units connected in serial. From the CV curves in Fig. 9(b), an enhanced potential range by MSC 400 units connected in serial can be provided. However, the current of four MSC 400 units connected in serial is inevitably reduced compared with the single MSC 400 unit due to the increase of serial resistance. Moreover, the MSC units perform stably even in the bent conditions as shown in Fig. 9(c), which is capable of satisfying various applications. As a result, the potential range can be improved by connecting MSC units in serial to meet the power and energy requirements.

D. Applications

With the in-planar layout and ideal electrochemical performance, the serial MSC units show promising potentials to supply the wearable devices and low-power electronic systems (Fig. 10(a)), such as commercial light emitting diode (LED) and liquid crystal display (LCD). Due to the flexibility and portability, it could be directly attached to the

bended surface of device or placed on the pocket without occupying too much space. When fully charged to 4 V, the serial connected MSC unit is powerful enough to drive a calculator to perform a series of calculations stably for 10 minutes as shown in Fig. 10(b). In addition, it could also power wearable LED continuously with 1 minute as the warning label without external energy supply (Fig. 10(c)).

V. Conclusions

In summary, we propose a facile and scalable procedure for fabricating a freestanding solid-state MSC with superior characteristics of lightweight, flexibility, stabilization and excellent electrochemical performance. Combing the electrolyte transferring with laser patterning process, the MSC is configured with CNT/nanofibers interdigital fingers as electrodes, gold thin layer as the current collector and the PVA/H_3PO_4 gel electrolyte as the ion reservoir and flexible substrate. With the in-planar and electrolyte-substrate layout, the dimension of MSC could be greatly decreased. The entire device demonstrates excellent electrochemical behavior with a high capacitance and stable cycling performance according to the fact that the electrospinning nanofibers own large surface area and CNTs exhibit high conductivity. In order to investigate the relationship between the line-width and electrochemical performance, we optimize the line-width (200 μm) of the MSC unit, which shows reliable areal capacitance (15.6 mF/cm^2) and retains more than 83% performance after 2,000 charging/discharging cycles. Furthermore, the potential range of MSC unit could be improved through serial connection to meet the demands of various low-power electronic systems. Based on the superior performance and on-chip compatibility, the freestanding MSC can be performed as ideal energy storage unit combined with the energy harvesting device or micro sensors to produce a self-powered system. Therefore, such freestanding MSC performs significant advantages in MEMS-based technology and low-cost electronics, as well as wearable devices and flexible miniaturized energy systems.

Acknowledgment

The authors would like to thank the staff of the National Key Laboratory of Science and Technology on Micro/Nano Fabrication, Peking University, for their help on the fabrications, cooperation and assistance.

References

[1] J. H. Pikul, H. G. Zhang, J. Cho, P. V. Braun, and W. P. King, "High-power lithium ion microbatteries from interdigitated three-dimensional bicontinuousnanoporous electrodes," *Nature Commun.*, vol. 4, p. 1732, Apr. 2013.

[2] M. F. El-Kady and R. B. Kaner, "Scalable fabrication of high-power graphene micro-supercapacitors for flexible and on-chip energy storage," *Nature Commun.*, vol. 4, p. 1475, Feb. 2013.

[3] X. Cheng *et al.*, "A flexible large-area triboelectric generator by low-cost roll-to-roll process for location-based monitoring," *Sens. Actuators A, Phys.*, vol. 247, pp. 206–214, Aug. 2016.

[4] L. Dhakar, F. E. H. Tay, and C. Lee, "Development of a broadband triboelectric energy harvester with SU-8 micropillars," *J. Microelectromech. Syst.*, vol. 24, no. 1, pp. 91–99, Feb. 2015.

[5] H. Liu, C. J. Tay, C. Quan, T. Kobayashi, and C. Lee, "Piezoelectric MEMS energy harvester for low-frequency vibrations with wideband operation range and steadily increased output power," *J. Micromech. Microeng.*, vol. 20, no. 5, pp. 1131–1142, Oct. 2011.

[6] Y. Jia and A. A. Seshia, "Power optimization by mass tuning for MEMS piezoelectric cantilever vibration energy harvesting," *J. Microelectromech. Syst.*, vol. 25, no. 1, pp. 108–117, Feb. 2016.

[7] M. Han, Q. Yuan, X. Sun, and H. Zhang, "Design and fabrication of integrated magnetic MEMS energy harvester for low frequency applications," *J. Microelectromech. Syst.*, vol. 23, no. 1, pp. 204–212, Jan. 2014.

[8] K. Tao *et al.*, "A novel two-degree-of-freedom MEMS electromagnetic vibration energy harvester," *J. Micromech. Microeng.*, vol. 26, no. 3, p. 035020, Feb. 2016.

[9] B.-U. Hwang *et al.*, "Transparent stretchable self-powered patchable sensor platform with ultrasensitive recognition of human activities," *ACS Nano*, vol. 9, no. 9, pp. 8801–8810, Aug. 2015.

[10] Y. Song *et al.*, "Integrated self-charging power unit with flexible supercapacitor and triboelectric nanogenerator," *J. Mater. Chem. A*, vol. 4, no. 37, pp. 14298–14306, Oct. 2016.

[11] K. Kashyap, A. Kumar, M. T. Hou, and J. A. Yeh, "Sidewall nanotexturing for high rupture strength of silicon solar cells," *J. Microelectromech. Syst.*, vol. 24, no. 1, pp. 7–9, Feb. 2015.

[12] W. Yang, K. K. Lee, and S. Choi, "A laminar-flow based microbial fuel cell array," *Sens. Actuators A, Chem.*, vol. 243, pp. 292–297, May 2017.

[13] J. Chmiola, C. Largeot, P.-L. Taberna, P. Simon, and Y. Gogotsi, "Monolithic carbide-derived carbon films for micro-supercapacitors," *Science*, vol. 328, no. 5977, pp. 480–483, Apr. 2010.

[14] P. Simon and Y. Gogotsi, "Materials for electrochemical capacitors," *Nature Mater.*, vol. 7, no. 11, pp. 845–854, Nov. 2008.

[15] Y. Huang *et al.*, "Highly integrated supercapacitor-sensor systems via material and geometry design," *Small*, vol. 12, no. 25, pp. 3393–3399, Jun. 2016.

[16] P. Saenger, N. Devillers, K. Deschinkel, M. C. Pera, R. Couturier, and F. Gustin, "Optimization of electrical energy storage system sizing for an accurate energy management in an aircraft," *IEEE Trans. Veh. Technol.*, to be published, doi: 10.1109/TVT.2016.2617288.

[17] Y. Song *et al.*, "Highly compression-tolerant folded carbon nanotube/paper as solid-state supercapacitor electrode," *Micro Nano Lett.*, vol. 11, no. 10, pp. 586–590, Oct. 2016.

[18] C. Guo, H. Li, X. Zhang, H. Huo, and C. Xu, "3D porous CNT/MnO_2 composite electrode for high-performance enzymeless glucose detection and supercapacitor application," *Sens. Actuators B, Chem.*, vol. 206, pp. 407–414, Jan. 2015.

[19] J.-H. Sung, S.-J. Kim, S.-H. Jeong, E.-H. Kim, and K.-H. Lee, "Flexible micro-supercapacitors," *J. Power Sources*, vol. 162, no. 2, pp. 1467–1470, Sep. 2006.

[20] S. Li, X. Wang, H. Xing, and C. Shen, "Micro supercapacitors based on a 3D structure with symmetric graphene or activated carbon electrodes," *J. Micromech. Microeng.*, vol. 23, no. 11, p. 114013, Oct. 2013.

[21] K. Wang *et al.*, "An all-solid-state flexible micro-supercapacitor on a chip," *Adv. Energy Mater.*, vol. 1, no. 6, pp. 1068–1072, Sep. 2011.

[22] X. Pu *et al.*, "Wearable textile-based in-plane microsupercapacitors," *Adv. Energy Mater.*, vol. 6, no. 24, Aug. 2016.

[23] X. Liu, S. Chen, J. Pu, and X. Wang, "A flexible all-solid-state micro supercapacitor and its application in electrostatic energy management system," *J. Microelectromech. Syst.*, vol. 25, no. 5, pp. 929–936, Oct. 2016.

[24] X. Wang and S. Li, "Micro supercapacitors for energy storage, on-chip devices based on prototyping of patterned nanoporous carbon," in *Proc. 18th Int. Conf. Solid-State Sens., Actuators, Microsyst. (TRANSDUCERS)*, Jun. 2015, pp. 488–493.

[25] C. W. Ma, P. C. Huang, and Y. J. Yang, "A paper-like mi-cro-supercapacitor with patterned buckypaper electrodes using a novel vacuum filtration technique," in *Proc. IEEE 28th Int. Conf. Micro Electro Mech. Syst. (MEMS)*, Jan. 2015, pp. 1067–1070.

[26] M. Xue *et al.*, "Microfluidic etching for fabrication of flexible and all-solid-state micro supercapacitor based on MnO_2 nanoparticles," *Nanosc.*, vol. 3, no. 7, pp. 2703–2708, Mar. 2011.

[27] J. Ren *et al.*, "Twisting carbon nanotube fibers for both wire-shaped micro-supercapacitor and micro-battery," *Adv. Mater.*, vol. 25, no. 8, pp. 1155–1159, Feb. 2013.

[28] J. Yun *et al.*, "Stretchable patterned graphene gas sensor driven by integrated micro-supercapacitor array," *Nano Energy*, vol. 19, pp. 401–414, Jan. 2016.

[29] P. Huang *et al.*, "On-chip and freestanding elastic carbon films for micro-supercapacitors," *Science*, vol. 351, no. 6274, pp. 691–695, Feb. 2016.

[30] M. Gnerlich, E. Pomerantseva, K. Gregorczyk, D. Ketchum, G. Rubloff, and R. Ghodssi, "Solid flexible electrochemical supercapacitor using Tobacco mosaic virus nanostructures and ALD ruthenium oxide," *J. Micromech. Microeng.*, vol. 23, no. 11, p. 114014, Oct. 2013.
[31] Y. Wang, Y. Shi, C. X. Zhao, J. I. Wong, X. W. Sun, and H. Y. Yang, "Printed all-solid flexible microsupercapacitors: Towards the general route for high energy storage devices," *Nanotechnology*, vol. 25, no. 9, p. 094010, Feb. 2014.
[32] W. Si, C. Yan, Y. Chen, S. Oswald, L. Han, and O. G. Schmidt, "On chip, all solid-state and flexible micro-supercapacitors with high performance based on MnO_x/Au multilayers," *Energy Environ. Sci.*, vol. 6, no. 11, pp. 3218–3223, Jul. 2013.
[33] M. S. Kim, B. Hsia, C. Carraro, and R. Maboudian, "Flexible micro-supercapacitors from photoresist-derived carbon electrodes on flexible substrates," in *Proc. IEEE 27th Int. Conf. Micro Electro Mech. Syst. (MEMS)*, Jan. 2014, pp. 389–392.
[34] Y. Song *et al.*, "Freestanding solid-state micro-supercapacitor based on laser-patterned nanofibers," in *Proc. IEEE 30th Int. Conf. Micro Electro Mech. Syst. (MEMS)*, Jan. 2017, pp. 809–812.
[35] B. E. Conway, *Electrochemical Supercapacitor: Scientific Fundamentals and Technological Applications*. New York, NY, USA: Kluwer, 1999.
[36] X. Lu, M. Yu, G. Wang, Y. Tong, and Y. Li, "Flexible solid-state supercapacitors: Design, fabrication and applications," *Energy Environ. Sci.*, vol. 7, no. 7, pp. 2160–2181, Jul. 2014.
[37] B. Xie *et al.*, "Laser-processed graphene based micro-supercapacitors for ultrathin, rollable, compact and designable energy storage components," *Nano Energy*, vol. 26, pp. 276–285, Apr. 2016.
[38] C. Zhang, J. Xiao, L. Qian, S. Yuan, S. Wang, and P. Lei, "Planar integration of flexible micro-supercapacitors with ultrafast charge and discharge based on interdigital nanoporous gold electrodes on a chip," *J. Mater. Chem. A*, vol. 4, no. 24, pp. 9502–9510, Jun. 2016.

Yu Song received the B.S. degree in electronic science and technology from the Huazhong University of Science and Technology, Wuhan, China, in 2015. He is currently pursuing the Ph.D. degree with the National Key Laboratory of Nano/Micro Fabrication Technology, Peking University, Beijing, China. He majors in MEMS, and his research is focusing on supercapacitors and self-charging power system.

Xue-Xian Chen received the B.S. degree from the University of Electronic Science and Technology of China, Chengdu, in 2015. She is currently pursuing the Ph.D. degree with the National Key Laboratory of Nano/Micro Fabrication Technology, Peking University, Beijing, China. Her research interests mainly include design and fabrication of hybrid nanogenerator and electrospinning process.

Jin-Xin Zhang received the B.S. degree from the School of Electronics Engineering and Computer Science, Peking University, Beijing, China, in 2016, where he is currently pursuing the Ph.D. degree with the National Key Laboratory of Nano/Micro Fabrication Technology. His research interests mainly include electronic skin design and pressure sensor fabrication.

Xiao-Liang Cheng received the B.S. degree from the University of Electronic Science and Technology of China, Chengdu, in 2014. He is currently pursuing the Ph.D. degree with the National Key Laboratory of Nano/Micro Fabrication Technology, Peking University, Beijing, China. His research interests mainly include design and fabrication of nanogenerator and mechanical energy harvester.

Hai-Xia (Alice) Zhang (SM'10) received the Ph.D. degree in mechanical engineering from the Huazhong University of Science and Technology, Wuhan, China, 1998. She is currently a Professor with the Institute of Microelectronics, Peking University, Beijing, China. She joined the Faculty of the Institute of Microelectronics in 2001 after finishing her Post-Doctoral Research at Tsinghua University. Her research interests include MEMS design and fabrication technology, SiC MEMS, and microenergy technology. She was a recipient of the National Invention Award of Science and Technology in 2006. She has served as the General Chair of the IEEE NEMS 2013 Conference and the Organizing Chair of Transducers'11. As the Founder of the International Contest of Applications in Network of Things, she has been organizing this world-wide event since 2007.